The Galaxy's Gas Content Regulated by the Dark Matter Halo Mass Results in a Superlinear $M_{\rm BH}$–$M_\star$ Relation

I. Delvecchio[1,2,9] , E. Daddi[1] , F. Shankar[3] , J. R. Mullaney[4] , G. Zamorani[2] , J. Aird[5] , E. Bernhard[4], A. Cimatti[6,7] , D. Elbaz[1] , M. Giavalisco[8] , and L. P. Grimmett[4]

[1] CEA, IRFU, DAp, AIM, Université Paris-Saclay, Université Paris Diderot, Sorbonne Paris Cité, CNRS, F-91191 Gif-sur-Yvette, France; ivan.delvecchio@cea.fr
[2] INAF—Osservatorio di Astrofisica e Scienza dello Spazio, via Gobetti 93/3, I-40129, Bologna, Italy
[3] Department of Physics and Astronomy, University of Southampton, Highfield SO17 1BJ, UK
[4] Department of Physics and Astronomy, The University of Sheffield, Hounsfield Road, Sheffield S3 7RH, UK
[5] Department of Physics & Astronomy, University of Leicester, University Road, Leicester LE1 7RJ, UK
[6] University of Bologna, Department of Physics and Astronomy (DIFA), Via Gobetti 93/2, I-40129, Bologna, Italy
[7] INAF—Osservatorio Astrofisico di Arcetri, Largo E. Fermi 5, I-50125, Firenze, Italy
[8] Department of Astronomy, University of Massachusetts Amherst, 710 North Pleasant Street, Amherst, MA 01003-9305, USA

Abstract

Supermassive black holes (SMBHs) are tightly correlated with their hosts, but the origin of such connection remains elusive. To explore the cosmic buildup of this scaling relation, we present an empirically motivated model that tracks galaxy and SMBH growth down to $z = 0$. Starting from a random mass seed distribution at $z = 10$, we assume that each galaxy evolves on the star-forming "main sequence" (MS) and each BH follows the recently derived stellar mass ($M_\star$) dependent ratio between BH accretion rate and star formation rate, going as BHAR/SFR $\propto M_\star^{0.73[+0.22,-0.29]}$. Our simple recipe naturally describes the BH–galaxy buildup in two stages. At first, the SMBH lags behind the host that evolves along the MS. Later, as the galaxy grows in $M_\star$, our $M_\star$-dependent BHAR/SFR induces a superlinear BH growth, as $M_{\rm BH} \propto M_\star^{1.7}$. According to this formalism, smaller BH seeds increase their relative mass faster and earlier than bigger BH seeds, at fixed $M_\star$, thus setting along a gradually tighter $M_{\rm BH}$–$M_\star$ locus toward higher $M_\star$. Assuming reasonable values of the radiative efficiency $\epsilon \sim 0.1$, our empirical trend agrees with both high-redshift model predictions and intrinsic $M_{\rm BH}$–$M_\star$ relations of local BHs. We speculate that the observed nonlinear BH–galaxy buildup is reflected in a twofold behavior with dark matter halo mass ($M_{\rm DM}$), displaying a clear turnover at $M_{\rm DM} \sim 2 \times 10^{12}\ M_\odot$. While supernovae-driven feedback suppresses BH growth in smaller halos (BHAR/SFR $\propto M_{\rm DM}^{1.6}$), above the $M_{\rm DM}$ threshold cold gas inflows possibly fuel both BH accretion and star formation in a similar fashion (BHAR/SFR $\propto M_{\rm DM}^{0.3}$).

Unified Astronomy Thesaurus concepts: Active galaxies (17); Galaxy evolution (594); AGN host galaxies (2017); Galaxy dark matter halos (1880); Supermassive black holes (1663)

1. Introduction

How supermassive black holes (SMBHs) formed and evolved with cosmic time is one of the most debated issues in modern astrophysics. One of the best-known pieces of evidence supporting coevolution between SMBHs and their host galaxies is the observed relationship at $z \sim 0$ between SMBH mass ($M_{\rm BH}$) and several properties of galaxy bulges: stellar velocity dispersion (σ_*), stellar bulge mass ($M_{\rm bulge}$), and dark matter halo mass ($M_{\rm DM}$; e.g., Magorrian et al. 1998; Ferrarese & Merritt 2000; Gebhardt et al. 2000; Häring & Rix 2004; Gültekin et al. 2009).

Such a tight (scatter $\sim$0.3 dex) correlation is currently interpreted as the outcome of a long-term balance between feeding and feedback processes occurring in galaxy bulges and their central BHs (see a comprehensive review by Kormendy & Ho 2013).

Nevertheless, it is still unclear whether the local $M_{\rm BH}$–$M_{\rm bulge}$ relation observed for classical galaxy bulges ($M_{\rm BH}/M_{\rm bulge} < 1/200$; Kormendy & Ho 2013) evolves with redshift. Several studies targeting high-redshift quasars found BHs as massive as $10^9\ M_\odot$ at $z > 6$, when the universe was less than 1 Gyr old (Mortlock et al. 2011; Wu et al. 2015; Bañados et al. 2018; Vito et al. 2019). This suggests the presence of high-redshift

BHs that are *overmassive* ($M_{\rm BH}/M_\star > 1/100$) relative to local scaling relations, as found in local giant ellipticals (Lupi et al. 2019). Nevertheless, their $M_{\rm BH}$ measurements might be biased, since they rely on gas dynamical estimates on kiloparsec scales, which might not hold within the BH sphere of influence. An alternative scenario is that the galaxy stellar/halo mass primarily regulates the amount of cold gas available for triggering and sustaining the central SMBH growth (see Volonteri 2010 for a review). Investigating the relationship between BH accretion rate (BHAR) and star formation rate (SFR) is crucial to shed light on the connection between both phenomena at various epochs.

A pioneering study of Mullaney et al. (2012) first proposed the idea that SMBH and galaxy growth are synchronized at all times at a universal BHAR/SFR $\sim 10^{-3}$. Recently, much empirical evidence argued that the BHAR/SFR ratio increases with $M_\star$ (Rodighiero et al. 2015; Yang et al. 2018; Aird et al. 2019). This was independently corroborated in Delvecchio et al. (2019, hereafter D19), via modeling the observed AGN X-ray luminosity function (XLF; Aird et al. 2015). In this Letter, we explore the implications on the cosmic SMBH growth resulting from an $M_\star$-dependent BHAR/SFR trend. In particular, assuming a seed distribution for both $M_{\rm BH}$ and galaxy $M_\star$ starting at very high redshift ($z = 10$), we let it evolve following the above trend. Finally, we compare their

---
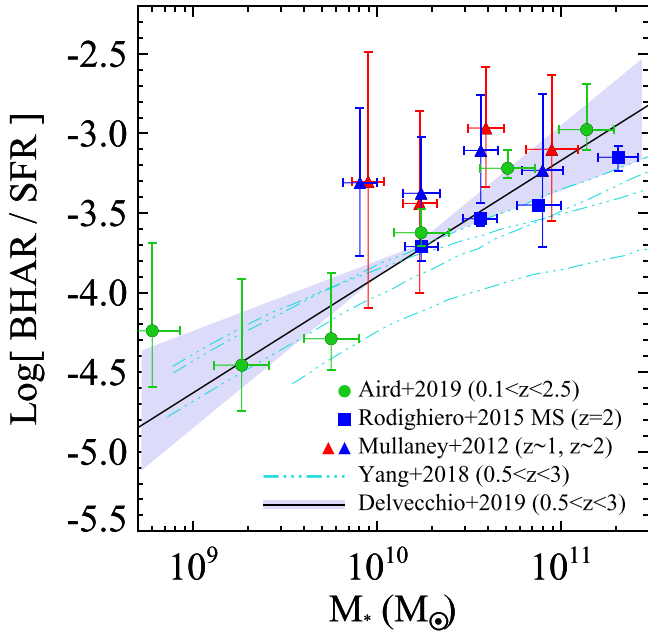
Figure 1. Compilation of various mean BHAR/SFR trends with $M_\star$ proposed in the literature. Empirical relations for star-forming galaxies are taken from Mullaney et al. (2012, $z \sim 1$ and $z \sim 2$, red and blue triangles, respectively), Rodighiero et al. (2015, $z \sim 2$, blue squares), and Yang et al. (2018, dotted–dashed lines, increasing with redshift over $0.5 < z < 3$). Data points from Aird et al. (2019, green circles) are averaged over the BHAR/SFR distributions across $0.1 < z < 2.5$. Our recent trend (D19, black solid line) was obtained by reproducing the observed XLF of AGN at $0.5 < z < 3$, yielding BHAR/SFR $\propto M_\star^{0.73[+0.22, -0.29]}$ at the $\pm 1\sigma$ confidence level (gray shaded area).

final mass buildup with observed scaling relations at $z = 0$ and state-of-the-art cosmological simulations at higher redshifts.

Throughout this Letter, we adopt a Chabrier (2003) initial mass function (IMF) and a flat cosmology with $\Omega_m = 0.30$, $\Omega_\Lambda = 0.70$, and $H_0 = 70 \, \mathrm{km \, s^{-1} \, Mpc^{-1}}$.

2. Our Empirically Motivated Toy Model

D19 successfully reproduced the observed AGN XLF (Aird et al. 2015) since $z \sim 3$, disentangling the relative contribution of main-sequence (MS) and starburst (SB) galaxies. The XLF was modeled as the convolution between the galaxy $M_\star$ function and a set of "specific BHAR" (s-BHAR = BHAR/$M_\star \propto L_X/M_\star$; see Aird et al. 2012) distributions that were normalized to match a number of empirical BHAR/SFR trends. From the derived XLF, we directly constrained the typical BHAR/SFR ratio to scale positively with $M_\star$, as BHAR/SFR $\propto M_\star^{0.73[+0.22, -0.29]}$, and roughly independent of redshift at $0.5 < z < 3$ (e.g., Aird et al. 2019). While extrapolating this BHAR/SFR trend at $z > 3$ might suffer from uncertainties, this finding suggests that SMBHs and their hosts do not grow in lockstep over cosmic time. Figure 1 displays our BHAR/SFR trend with $M_\star$ (black solid line) and the corresponding $\pm 1\sigma$ scatter (gray shaded area). For comparison, in Figure 1 we report other data and trends from the literature (Mullaney et al. 2012; Rodighiero et al. 2015; Yang et al. 2018; Aird et al. 2019) at various redshifts. In particular, Yang et al. (2018) argue for a flatter BHAR/SFR trend with $M_\star$, and slightly increasing with redshift. However, we stress that the redshift dependence is, at least partly, a consequence of the $M_\star$-independent MS relation assumed by the authors (from Behroozi et al. 2013). The absence of a

bending toward high $M_\star$ leads to slightly higher SFR, therefore lower BHAR/SFR relation, especially at low redshift where the flattening is stronger (e.g., Schreiber et al. 2015). Therefore, under the assumption of a bending MS, the above studies are all consistent with a redshift-invariant BHAR/SFR ratio.

2.1. Initial Mass Seed Distributions

In order not to bias ourselves to any prior seed distribution, we start with a uniform sample of 1000 seeds formed at $z = 10$, with masses $M_{\mathrm{BH}} = 10^{2-6} \, M_\odot$ and $M_\star = 10^{6-10} \, M_\odot$. Such an input grid spans a wide range of $M_{\mathrm{BH}}/M_\star$, covering the mass range predicted by the main BH seed formation channels (Begelman & Rees 1978): (i) PopIII stars remnants ($\sim 10^2 \, M_\odot$); (ii) stellar dynamical collapse ($\sim 10^3 \, M_\odot$); (iii) gas dynamical collapse ($\sim 10^{5-6} \, M_\odot$). Taking a higher (lower) initial redshift would simply yield slightly smaller (larger) $M_\star$ at $z = 0$. Independently of this, their M_{BH} estimates would scale accordingly (based on the BHAR/SFR trend with $M_\star$), keeping our final results and conclusions unchanged.

2.2. Setting Galaxy $M_\star$ Growth

For each galaxy $M_\star$ and redshift, we assign the corresponding SFR by following the MS relation of Schreiber et al. (2015), rescaled to a Chabrier (2003) IMF. The MS scatter was propagated on the derived SFR by following a lognormal distribution with 1σ dispersion of 0.3 dex (Schreiber et al. 2015). The cumulative $M_\star$ is simply calculated as the time integral of the SFR. We acknowledge that a more detailed treatment of the $M_\star$ buildup would require a correction for stellar mass losses (Leitner & Kravtsov 2011), which would slightly lower our integrated $M_\star$, and consequently our M_{BH}, without affecting the overall trend. In fact, our main goal is to track the cosmic assembly of the M_{BH}–$M_\star$ *slope and normalization* at various epochs, not to match the observed galaxy $M_\star$ distribution at each redshift.

2.3. Setting BH Growth

Each BH seed is assumed to gain mass via gas accretion (Soltan 1982) at a fixed radiative efficiency $\epsilon = 0.1$ (e.g., Marconi et al. 2004). Because of an $M_\star$-dependent BHAR/SFR ratio, we translate the corresponding SFR into a *long-term average* BHAR, at each $M_\star$. Based on this formalism, we determine the cumulative accreted SMBH mass since $z = 10$ as

$$M_{\mathrm{BH}}|_{z=0} = \int_{z=10}^{z=0} \mathrm{BHAR}|_{M_\star(z')} \cdot \frac{dt'}{dz'} \, dz' + M_{\mathrm{BH}}|_{z=10}. \quad (1)$$

The corresponding Eddington ratio λ_{EDD}, at each $M_\star$ (and redshift), is calculated as

$$\lambda_{\mathrm{EDD}}|_{M_\star(z')} = 4.41 \cdot 10^8 \cdot \frac{\epsilon}{1 - \epsilon} \cdot \frac{\mathrm{BHAR}|_{M_\star(z')}}{M_{\mathrm{BH}}/M_\odot}. \quad (2)$$

We iterate the above procedure down to $z = 0$ with a redshift step of 0.1.

3. Results

Exploring the cosmic buildup induced by an $M_\star$-dependent BHAR/SFR ratio is paramount for understanding whether the galaxy (halo) governs SMBH growth by setting the available amount of gas for fueling SF and BH accretion, or instead if early AGN feedback controls the amount of cold star-forming gas that fuels galaxy growth (Volonteri 2010).

Delvecchio et al.
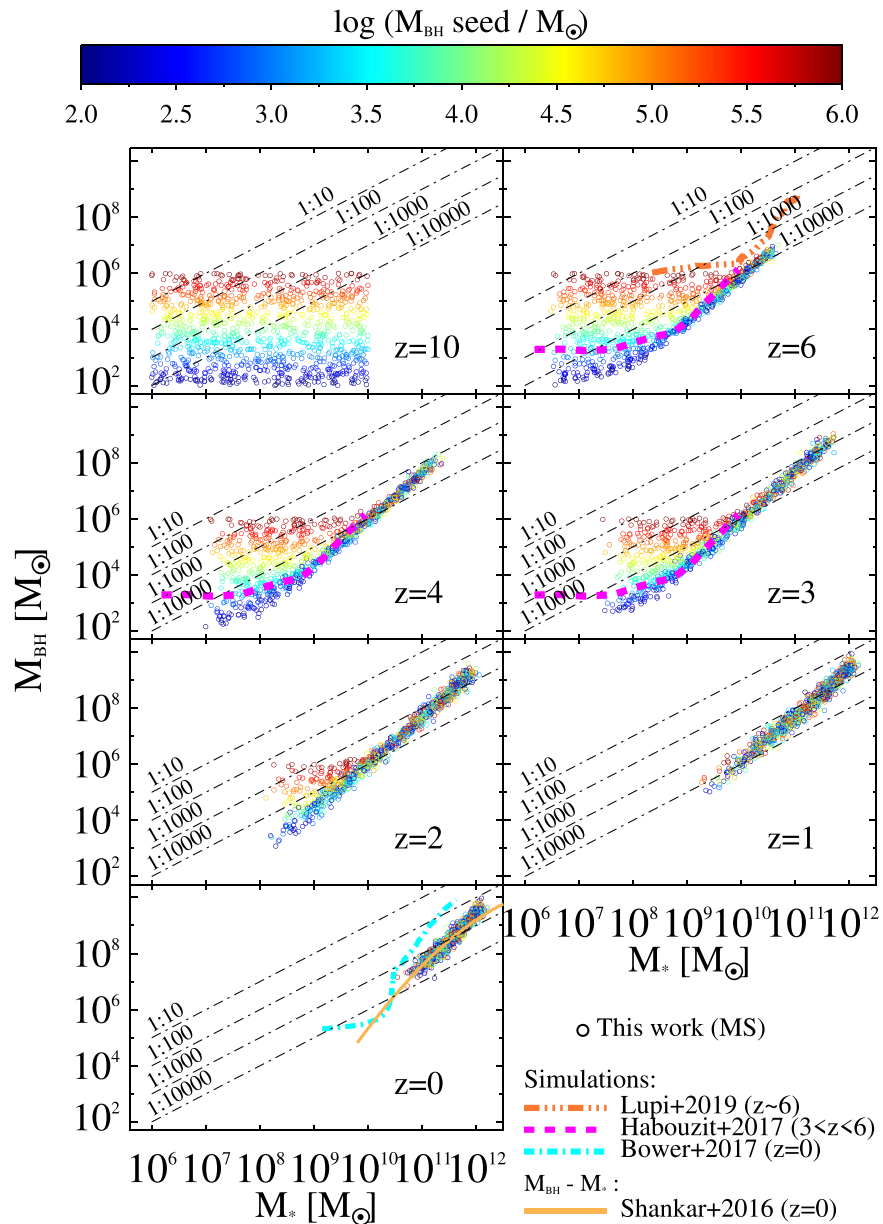
Figure 2. Cosmic buildup of SMBH and galaxy mass implied by our $M_\star$-dependent BHAR/SFR trend (open circles). We assume uniform M_{BH} and $M_\star$ seed distributions at $z_f = 10$, spanning the ranges $10^2 < M_{BH} < 10^6$ and $10^6 < M_\star < 10^{10}\ M_\odot$, respectively (top left panel). The color bar indicates the seed M_{BH} distribution at z_f. Dotted–dashed lines mark various $M_{BH}/M_\star$ ratios. We track the evolution of $M_\star$ and M_{BH} for MS galaxies (circles), incorporating the scatter of the MS relation and the uncertainties on the assumed BHAR/SFR trend. For comparison, we show predictions of an SB galaxy at $z \sim 6$ (Lupi et al. 2019, orange dotted–dashed line), and of normal star-forming galaxies (Habouzit et al. 2017, magenta dotted line at $3 < z < 6$; Bower et al. 2017, cyan dotted–dashed line at $z = 0$). We also show the proposed debiased M_{BH}–$M_\star$ relation at $z = 0$ (Shankar et al. 2016, yellow solid line). The absence of galaxies with $M_\star < 10^{10}\ M_\odot$ at $z = 0$ is simply attributable to our limited $M_\star$ grid at $z = 10$.

Figure 2 displays the evolution of 1000 $M_\star$ and M_{BH} seeds (circles) since $z_f = 10$, resulting from our empirical $M_\star$-dependent BHAR/SFR (D19). The color bar indicates the seed M_{BH} distribution. For convenience, dotted–dashed lines mark various $M_{BH}/M_\star$ ratios. We track the evolution of $M_\star$ and M_{BH} while propagating, at each time step, the dispersion of the MS relation and the uncertainty on the BHAR/SFR trend.

The positive BHAR/SFR relation with $M_\star$ suggests that SMBH accretion and star formation do *not* proceed in lockstep at all cosmic epochs, whereas their buildup comes in two stages (Figure 2).

Because of our $M_\star$-dependent BHAR/SFR trend, in small $M_\star$ galaxies the BHAR is quite low relative to the SFR; therefore, the

SMBH lags behind the galaxy. As the galaxy steadily grows in $M_\star$, the BHAR is progressively enhanced relative to the SFR. In this regime, the BH grows superlinearly as $M_{BH} \propto M_\star^{1.7}$, setting along a gradually tighter M_{BH}–$M_\star$ locus toward higher $M_\star$. This is because two BHs with different M_{BH} but same galaxy $M_\star$ have the same BHAR. Hence, while the *absolute* BH mass gained per unit time is the same, a smaller BH seed will increase its *relative* mass by a much larger factor than a bigger BH seed.

Therefore, the seed $M_\star$ is the key quantity that *attracts* all seeds toward a superlinear slope, above a critical $M_\star$ value (Figure 2). Instead, the seed M_{BH} is the parameter that sets the corresponding $M_\star$ threshold, increasing with seed M_{BH}, above which any prior BH seed dependence is lost.
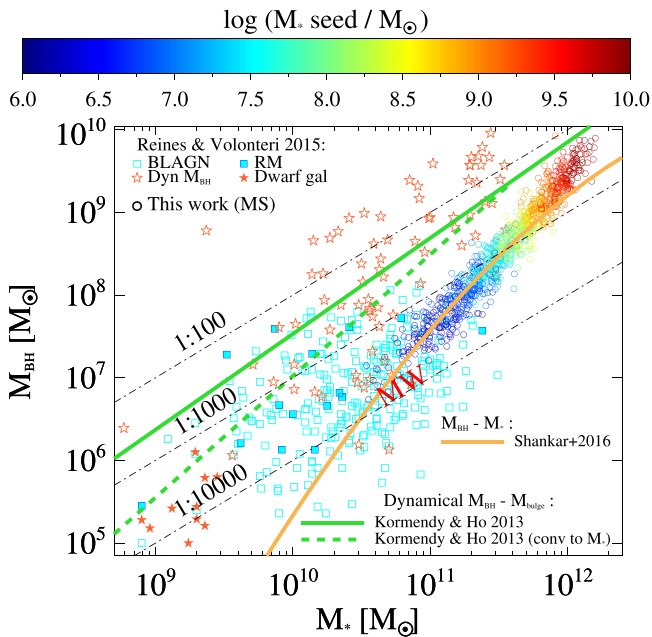
Figure 3. Final M_{BH}–$M_\star$ relation at $z = 0$ determined by our $M_\star$-dependent BHAR/SFR. The color bar indicates the seed $M_\star$ distribution at z_f. For comparison, we show the local relation from Kormendy & Ho (2013), both with M_{bulge} (green solid line) and converted to total $M_\star$ (green dashed line). Our MS wedge agrees remarkably well with the proposed debiased M_{BH}–$M_\star$ trend (Shankar et al. 2016, yellow solid line) and with the virial M_{BH} estimates for BLAGN (Reines & Volonteri 2015, empty squares). For completeness, we report M_{BH}–$M_\star$ estimates collected from Reines & Volonteri (2015) for reverberation mapping AGN (RM, filled squares), dynamical M_{BH} measurements (empty stars), and dwarf galaxies (filled stars). The tag "MW" marks the mass measurements for the Milky Way.

For comparison, Figure 2 reports predictions from cosmological simulations of an SB galaxy at $z \sim 6$ (Lupi et al. 2019, orange dotted–dashed line), and of normal star-forming galaxies (Habouzit et al. 2017, magenta dotted line at $3 < z < 6$; Bower et al. 2017, cyan dotted–dashed line at $z = 0$). Lupi et al. (2019) used a cosmological simulation for studying the evolution of a quasar host-galaxy at $z \sim 6$–7, with seed $M_{BH} = 10^6 \, M_\odot$ at $z \gtrsim 10$. Instead, the model of Habouzit et al. (2017) explores the early growth ($3 < z < 8$) of lighter BH seeds, with $M_{BH} = 10^{2-3} \, M_\odot$. Finally, Bower et al. (2017) report the results from the EAGLE cosmological simulation (Schaye et al. 2015). All these models support strong supernovae-driven winds in the early phases of galaxy growth, that evacuate the gas around the central SMBH (Dubois et al. 2015), halting both BH and galaxy bulge growth. However, the rest of the galaxy keeps growing on the MS until it reaches a critical $M_\star$, increasing with seed M_{BH}. At this stage, the galaxy potential well is deep enough to retain the ejected gas, and to drive it more effectively toward the center. The BH grows superlinearly with $M_\star$ matching the proposed debiased M_{BH}–$M_\star$ relation (Shankar et al. 2016, yellow solid line; see Figure 3). This predicted scenario is qualitatively consistent with our empirical toy model predictions, as a natural consequence of an $M_\star$-dependent BHAR/SFR ratio. A noteworthy difference is that the above cosmological simulations do not directly link the BHAR to the host's properties, while our toy model assumes that BHAR depends exclusively on the galaxy's star-forming content.
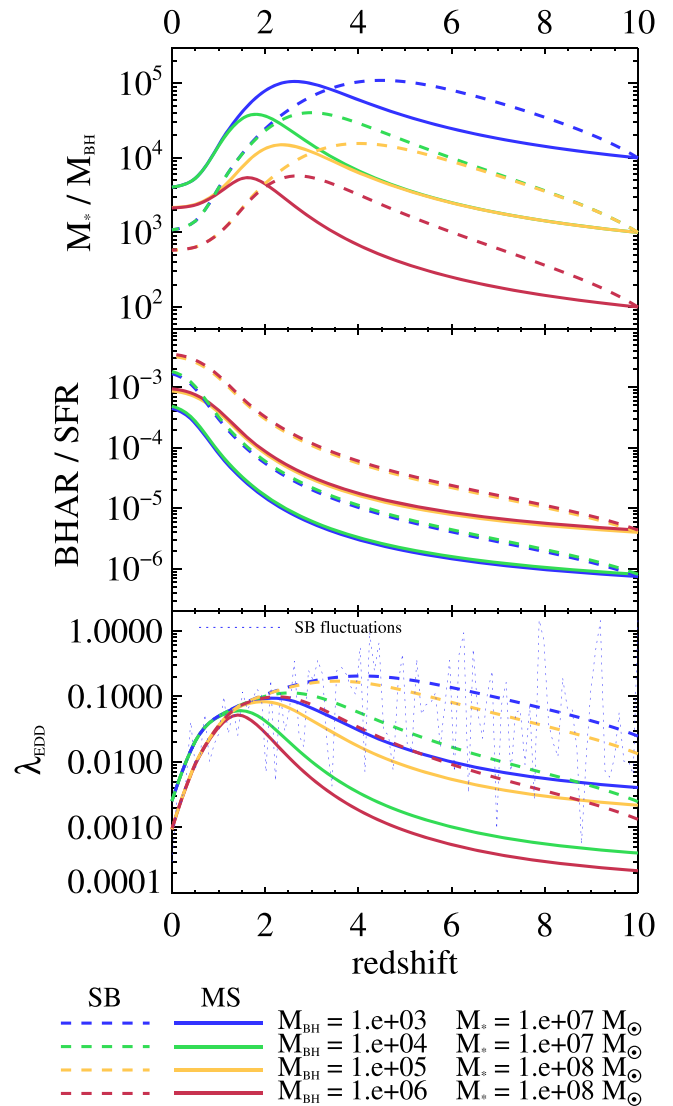
Figure 4. Redshift evolution of various SMBH- and galaxy-related parameters for four different seed masses (colored lines). The trends for MS and SB galaxies are highlighted with solid and dashed lines, respectively. Top panel: $M_{BH}/M_\star$ ratio. Middle panel: BHAR/SFR ratio. Bottom panel: Eddington ratio (λ_{EDD}). The blue dotted line marks the typical fluctuations in λ_{EDD} of an SB galaxy with seed $(M_{BH}, M_\star) = (10^3, 10^7) \, M_\odot$ (blue dashed line) when propagating the dispersion of the MS relation and the scatter of the assumed BHAR/SFR trend.

In Figure 3 we further test our empirical predictions at $z = 0$ against the local relation by Kormendy & Ho (2013), both with M_{bulge} (green solid line) and converted to total $M_\star$ (green dashed line), by applying a $M_\star$–dependent bulge-to-total (B/T) correction for local MS galaxies (Dimauro et al. 2018). Our MS wedge agrees remarkably well with the M_{BH}–$M_\star$ of Shankar et al. (2016, yellow solid line), suggesting that our long-term averaged BHAR/SFR trend is able to recover the intrinsic M_{BH}–$M_\star$ relation of MS galaxies. In addition, our trend fits very well the broad-line AGN (BLAGN) sample of Reines & Volonteri (2015), who exploited 262 single-epoch M_{BH} estimates down to $\approx 10^5 \, M_\odot$, for which they computed the total galaxy $M_\star$. This low-mass AGN sample contains moderate-luminosity AGN ($10^{41.5} < L_{AGN} < 10^{44.4} \, \mathrm{erg \, s^{-1}}$), hence significantly more common than previous quasars samples. The authors found a $10\times$ lower normalization than
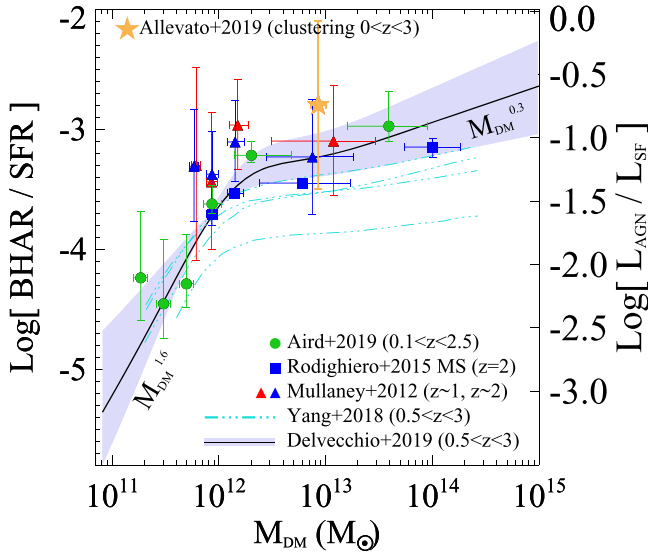
Figure 5. Compilation of various BHAR/SFR trends with M_{DM}, after applying the $M_\star$–M_{DM} conversion for star-forming galaxies (Behroozi et al. 2019) at $z = 1$. Symbols are the same shown in Figure 1. The right y-axis shows the equivalent AGN-to-galaxy bolometric output L_{AGN}/L_{SF}. The clear twofold trend suggests that M_{DM} might be crucial for explaining the nonlinear SMBH growth.

that inferred for dynamical M_{BH}–M_{bulge} trends of inactive elliptical galaxies (Kormendy & Ho 2013), which we interpret in the next section.

4. Discussion and Summary

Our findings corroborate the idea that galaxies and their SMBHs do not grow in lockstep at all times. Cosmological simulations predict that the SMBH first starves until the galaxy reaches a critical $M_\star \sim 10^{9-10}\ M_\odot$ (Bower et al. 2017; Habouzit et al. 2017; Lupi et al. 2019), corresponding to $M_{DM} \sim 10^{11-12}\ M_\odot$ (e.g., McAlpine et al. 2018). Later, they predict a superlinear BH growth toward $M_{BH}/M_\star \gtrsim 10^{-3}$ at $M_\star \gtrsim 10^{11}\ M_\odot$, in qualitative agreement with our findings.

The twofold trend predicted also by our toy model can be better visualized in Figure 4, which displays the cosmic evolution of $M_{BH}/M_\star$ (top panel), BHAR/SFR (middle panel), and λ_{EDD} (bottom panel) in MS galaxies (solid lines). Colors highlight representative cases with different seed masses. For completeness, we also show the extreme case of a continuous SB-like evolution (dashed lines), for which BH and galaxy growth proceed about $5\times$ faster than on the MS (Schreiber et al. 2015).

The typical $M_{BH}/M_\star$ ratio of MS galaxies (top panel) decreases from $z = 10$ until $z \sim 2$–3, and then rises toward $z = 0$. We note that smaller BH seeds increase their relative mass faster and earlier than bigger BH seeds, at fixed $M_\star$. Above a certain critical $M_\star$, increasing with seed M_{BH}, all seeds converge toward a similar (within a factor of two) $M_{BH}/M_\star$ ratio at $z = 0$. The evolution of SB galaxies shows instead a minimum at higher redshifts, as they reach the critical $M_\star$ on about $5\times$ shorter timescales ($\propto M_\star/SFR$) relative to MS analogs. For this reason, the BHAR/SFR ratio of SB galaxies appears systematically higher than for z-matched MS analogs (middle panel). We calculate the mean λ_{EDD} from Equation (2) and display its evolution with redshift (bottom panel). In MS

galaxies, the typical λ_{EDD} peaks at $1.5 < z < 2.5$, slightly increasing with decreasing M_{BH} seed. In comparison, SB galaxies reach a peak at higher redshifts ($2 < z < 4$). The blue dotted line indicates the typical fluctuations in λ_{EDD} of an SB galaxy with seed $(M_{BH}, M_\star) = (10^3, 10^7)\ M_\odot$ (blue dashed line) when propagating the dispersion of the MS relation and the scatter of the assumed BHAR/SFR trend. The amplitude of such fluctuations (similar also for the other mass seeds) suggests that SMBH accretion can vary over several orders of magnitude within the uncertainties, and it may occasionally reach Eddington-limited accretion in starbursting galaxies, consistently with high-redshift model predictions (e.g., Lupi et al. 2019).

The fact that BHAR is enhanced relative to SFR in the most massive galaxies might be also linked to the increasing compactness observed in star-forming galaxies toward higher $M_\star$ ($M_\star \propto R^{0.4}$; van der Wel et al. 2014). Indeed, a higher compactness might enhance the galaxy's ability to retain cold gas re-injected from stellar/AGN feedback, and eventually drive it within the BH sphere of influence.

In addition, environmental mechanisms linked to M_{DM} might help replenish and sustain BH–galaxy growth via inflows of pristine cold gas, predicted to be more effective in massive halos (Dekel et al. 2009). To test this, we adopt the $M_\star$-dependent $M_{DM}/M_\star$ ratio for star-forming galaxies from Behroozi et al. (2019) at $z = 1$,[10] and display the BHAR/SFR trend with M_{DM} in Figure 5. The nonlinear $M_\star$–M_{DM} conversion generates a strikingly twofold behavior that nicely resembles our empirical twofold BH–galaxy growth. In small DM halos supernovae-driven feedback suppresses BH growth (BHAR/SFR $\propto M_{DM}^{1.6}$) out to $M_{DM} \sim 2 \times 10^{12}\ M_\odot$, where baryons are most efficiently converted into stars. Above the turnover M_{DM}, AGN activity (exerting both positive and negative feedback) and cold gas inflows might enhance both BH accretion and galaxy star formation. At $M_{DM} \gtrsim 10^{13}\ M_\odot$ the BHAR/SFR ratio flattens out (BHAR/SFR $\propto M_{DM}^{0.3}$), possibly due to shock-heated gas within the DM halo (Dekel et al. 2009). We find a good agreement with the average BHAR/SFR and M_{DM} measurements obtained from clustering of X-ray AGN at $0 < z < 3$ (Allevato et al. 2019, yellow star). Therefore, we speculate that M_{DM} might be the leading physical driver of the observed nonlinear BH–galaxy growth.

In Figure 5 we link the BHAR/SFR ratio to the AGN-to-galaxy bolometric output (L_{AGN}/L_{SF}, right y-axis), assuming that BH accretion occurs with $\epsilon = 0.1$. Instead, the galaxy bolometric power arising from star formation (L_{SF}) is calculated by converting the (obscured) SFR into rest-frame 8–1000 μm luminosity, via a Kennicutt (1998) scaling factor. While L_{AGN} is always subdominant relative to L_{SF}, their ratio increases and displays a turnover in M_{DM} at $L_{AGN}/L_{SF} \approx 10\%$, above which it slowly approaches energy equipartition. Adding some contribution from unobscured star formation, particularly toward low $M_\star$, would strengthen the resulting trends. We also note that assuming L_X-dependent bolometric corrections for deriving the BHAR (e.g., Lusso et al. 2012) would further steepen the resulting BHAR/SFR trend with $M_\star$, amplifying the twofold behavior with M_{DM}.

We acknowledge that our toy model is not able to reproduce BHs as massive as $10^{9-10}\ M_\odot$ already at $z \sim 6$ (e.g., Mortlock et al. 2011), even in the unlikely scenario of continuous SB-like

---

[10] Taking the conversion at a different intermediate redshift would not affect our conclusions.

evolution since $z = 10$. Indeed, our toy model would form BHs with $M_{BH} \lesssim 10^8\ M_\odot$ at $z = 6$, but the galaxy would overgrow in $M_\star$ if extrapolating down to $z = 0$ (Renzini 2009). As for local dynamical M_{BH} measurements, we believe that high-redshift observations are also likely biased toward the brightest AGN and most massive BHs that swamp the host-galaxy light, a critical condition to ensure reliable M_{BH} estimates. Therefore, we argue that such quasars at $z \sim 6$, if their M_{BH} are not overestimated (but see Mejía-Restrepo et al. 2018), must have grown at a BHAR/SFR ratio about $10\times$ higher than that assumed in this work. If such a notable ratio was followed by the overall AGN population at $z \sim 6$, we would severely overestimate the observed XLF (D19) and the declining BHAR density constrained by deep X-ray data at $z > 3$ (Vito et al. 2018). This leads us believe that the most massive quasars at $z \sim 6$ followed very peculiar and uncommon evolutionary paths.

At $z = 0$, Figure 3 shows that our toy model agrees well with proposed debiased M_{BH}–$M_\star$ relations (Shankar et al. 2016) and representative AGN samples (Reines & Volonteri 2015). Nevertheless, we note a significant ($>10\times$) discrepancy at $M_\star \lesssim 10^{11}\ M_\odot$ relative to empirical M_{BH}–M_{bulge} relations based on dynamical M_{BH} measurements (Kormendy & Ho 2013). This apparent conflict might arise for multiple reasons: (i) The local M_{BH}–M_{bulge} relation is likely biased toward the largest BHs hosted within massive quiescent systems, for which the BH sphere of influence can be spatially resolved (Gültekin et al. 2009; Shankar et al. 2016, 2019). This biases the intrinsic M_{BH}–M_{bulge} relation toward a flatter slope and higher normalization (Volonteri & Stark 2011). (ii) While in the most massive galaxies $M_{bulge} \approx M_\star$, at $M_\star = 10^{10}\ M_\odot$ the B/T decreases to ≈ 0.3 for local MS galaxies (Dimauro et al. 2018). This behavior causes an $M_\star$-dependent steepening of the M_{BH}–M_{bulge} relation (green dashed line in Figure 3), though not crucial for reconciling the observed difference. (iii) A significant fraction of SMBH accretion might be heavily obscured, thus inaccessible via X-ray observations. However, this elusive contribution might boost the average BHAR by at most a factor of $\lesssim 2$, thus not filling the observed gap at low $M_\star$ (Comastri et al. 2015). (iv) The average radiative efficiency might be much lower than $\epsilon = 0.1$ (possibly $M_\star$ dependent). As a consequence, the corresponding mass accreted by SMBHs at fixed luminosity would be higher. However, the lowest theoretically expected value of $\epsilon = 0.06$ (Novikov & Thorne 1973) proves still insufficient to justify the observed discrepancy. Therefore, we favor the combination of points (i) and (ii) as possible reasons to explain the conflicting M_{BH}–$M_\star$ trends at $z = 0$.

In conclusion, the proposed empirically motivated BHAR/SFR trend with $M_\star$ (D19) enables us to describe the cosmic SMBH–galaxy assembly in normal SF galaxies, in agreement with high-z cosmological simulations and intrinsic M_{BH}–$M_\star$ relations at $z = 0$. Our study suggests that the DM halo mass primarily regulates the amount of cold gas available for triggering and sustaining the cosmic nonlinear BH–galaxy growth.

ORCID iDs

I. Delvecchio ◉ https://orcid.org/0000-0001-8706-2252
E. Daddi ◉ https://orcid.org/0000-0002-3331-9590
F. Shankar ◉ https://orcid.org/0000-0001-8973-5051
J. R. Mullaney ◉ https://orcid.org/0000-0002-3126-6712
G. Zamorani ◉ https://orcid.org/0000-0002-2318-301X
J. Aird ◉ https://orcid.org/0000-0003-1908-8463
A. Cimatti ◉ https://orcid.org/0000-0002-4409-5633
D. Elbaz ◉ https://orcid.org/0000-0002-7631-647X
M. Giavalisco ◉ https://orcid.org/0000-0002-7831-8751

References

Aird, J., Alexander, D. M., Ballantyne, D. R., et al. 2015, ApJ, 815, 66
Aird, J., Coil, A. L., & Georgakakis, A. 2019, MNRAS, 484, 4360
Aird, J., Coil, A. L., Moustakas, J., et al. 2012, ApJ, 746, 90
Allevato, V., Viitanen, A., Finoguenov, A., et al. 2019, A&A, in press (arXiv:1910.08084)
Bañados, E., Venemans, B. P., Mazzucchelli, C., et al. 2018, Natur, 553, 473
Begelman, M. C., & Rees, M. J. 1978, MNRAS, 185, 847
Behroozi, P., Wechsler, R. H., Hearin, A. P., et al. 2019, MNRAS, 488, 3143
Behroozi, P. S., Wechsler, R. H., & Conroy, C. 2013, ApJ, 770, 57
Bower, R. G., Schaye, J., Frenk, C. S., et al. 2017, MNRAS, 465, 32
Chabrier, G. 2003, ApJL, 586, L133
Comastri, A., Gilli, R., Marconi, A., Risaliti, G., & Salvati, M. 2015, A&A, 574, L10
Dekel, A., Birnboim, Y., Engel, G., et al. 2009, Natur, 457, 451
Delvecchio, I., Daddi, E., Aird, J., et al. 2019, ApJ, submitted
Dimauro, P., Huertas-Company, M., Daddi, E., et al. 2018, MNRAS, 478, 5410
Dubois, Y., Volonteri, M., & Silk, J. 2015, MNRAS, 452, 1502
Ferrarese, L., & Merritt, D. 2000, ApJL, 539, L9
Gebhardt, K., Bender, R., Bower, G., et al. 2000, ApJL, 539, L13
Gültekin, K., Richstone, D. O., Gebhardt, K., et al. 2009, ApJ, 698, 198
Habouzit, M., Volonteri, M., & Dubois, Y. 2017, MNRAS, 468, 3935
Häring, N., & Rix, H.-W. 2004, ApJL, 604, L89
Kennicutt, R. C., Jr. 1998, ApJ, 498, 541
Kormendy, J., & Ho, L. C. 2013, ARA&A, 51, 511
Leitner, S. N., & Kravtsov, A. V. 2011, ApJ, 734, 48
Lupi, A., Volonteri, M., Decarli, R., et al. 2019, MNRAS, 488, 4004
Lusso, E., Comastri, A., Simmons, B. D., et al. 2012, MNRAS, 425, 623
Magorrian, J., Tremaine, S., Richstone, D., et al. 1998, AJ, 115, 2285
Marconi, A., Risaliti, G., Gilli, R., et al. 2004, MNRAS, 351, 169
McAlpine, S., Bower, R. G., Rosario, D. J., et al. 2018, MNRAS, 481, 3118
Mejía-Restrepo, J. E., Lira, P., Netzer, H., et al. 2018, NatAs, 2, 63
Mortlock, D. J., Warren, S. J., Venemans, B. P., et al. 2011, Natur, 474, 616
Mullaney, J. R., Daddi, E., Béthermin, M., et al. 2012, ApJL, 753, L30
Novikov, I. D., & Thorne, K. S. 1973, in Black Holes (Les Astres Occlus), ed. C. DeWitt & B. DeWitt (New York: Gordon and Breach), 343
Reines, A. E., & Volonteri, M. 2015, ApJ, 813, 82
Renzini, A. 2009, MNRAS, 398, L58
Rodighiero, G., Brusa, M., Daddi, E., et al. 2015, ApJL, 800, L10
Schaye, J., Crain, R. A., Bower, R. G., et al. 2015, MNRAS, 446, 521
Schreiber, C., Pannella, M., Elbaz, D., et al. 2015, A&A, 575, A74
Shankar, F., Bernardi, M., Richardson, K., et al. 2019, MNRAS, 485, 1278
Shankar, F., Bernardi, M., Sheth, R. K., et al. 2016, MNRAS, 460, 3119
Soltan, A. 1982, MNRAS, 200, 115
van der Wel, A., Franx, M., van Dokkum, P. G., et al. 2014, ApJ, 788, 28
Vito, F., Brandt, W. N., Bauer, F. E., et al. 2019, A&A, 628, L6
Vito, F., Brandt, W. N., Yang, G., et al. 2018, MNRAS, 473, 2378
Volonteri, M. 2010, A&ARv, 18, 279
Volonteri, M., & Stark, D. P. 2011, MNRAS, 417, 2085
Wu, X.-B., Wang, F., Fan, X., et al. 2015, Natur, 518, 512
Yang, G., Brandt, W. N., Vito, F., et al. 2018, MNRAS, 475, 1887